Facile hydrothermal synthesis of tubular kapok fiber/MnO_2 hybrid composites and application in supercapacitors

Weibing Xu[a,b] Bin Mu,[a] Wenbo Zhang[a] and Aiqin Wang,[a]*

[a]* *State Key Laboratory of Solid Lubrication, Center of Eco-Materials and Green Chemistry, Lanzhou Institute of Chemical Physics, Chinese Academy of Sciences, Lanzhou 730000, China.*

[b] *University of the Chinese Academy of Sciences, Beijing 100049, P.R. China.*

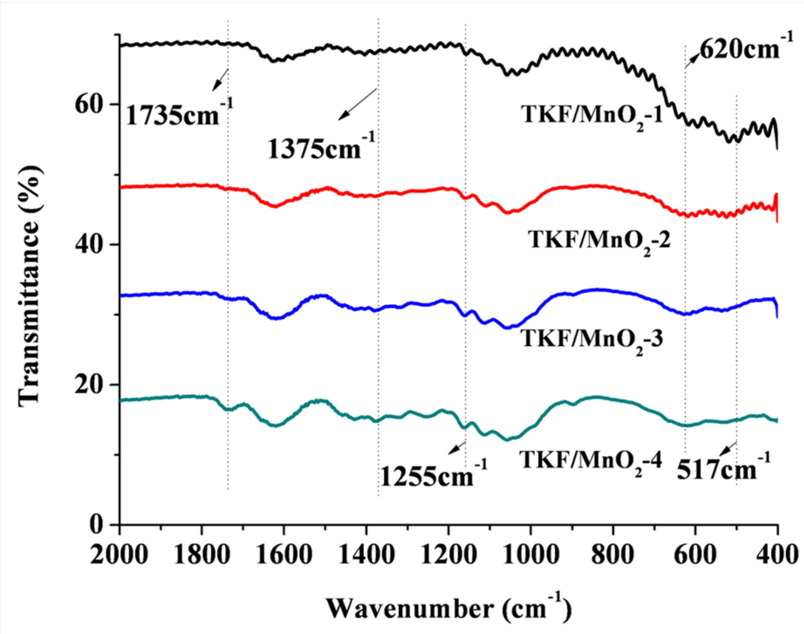

Fig.S1 FTIR spectra of TKF/MnO_2-1, TKF/MnO_2-2, TKF/MnO_2-3 and TKF/MnO_2-4 composites

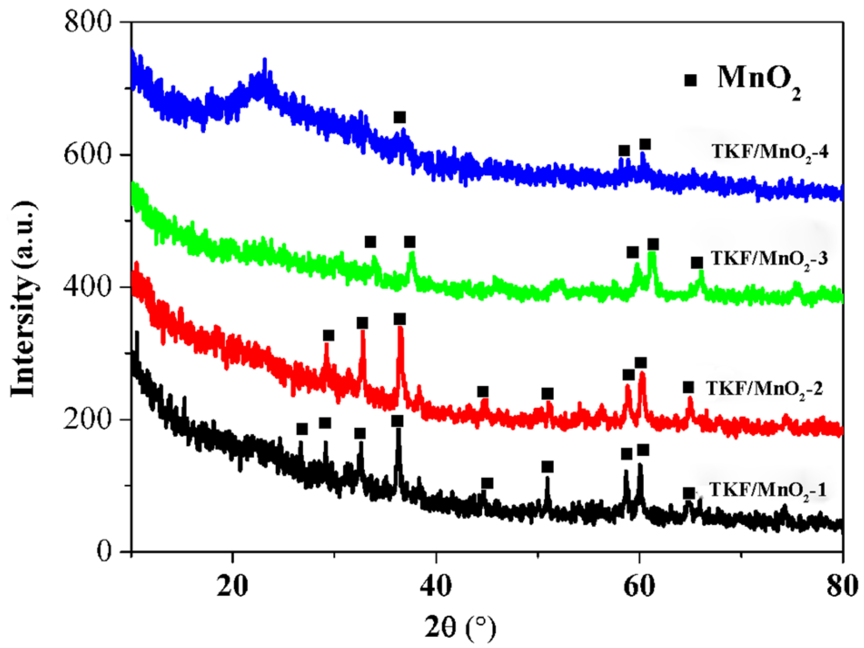

Fig.S2 XRD spectra of TKF/MnO_2-1, TKF/MnO_2-2, TKF/MnO_2-3 and TKF/MnO_2-4 composites

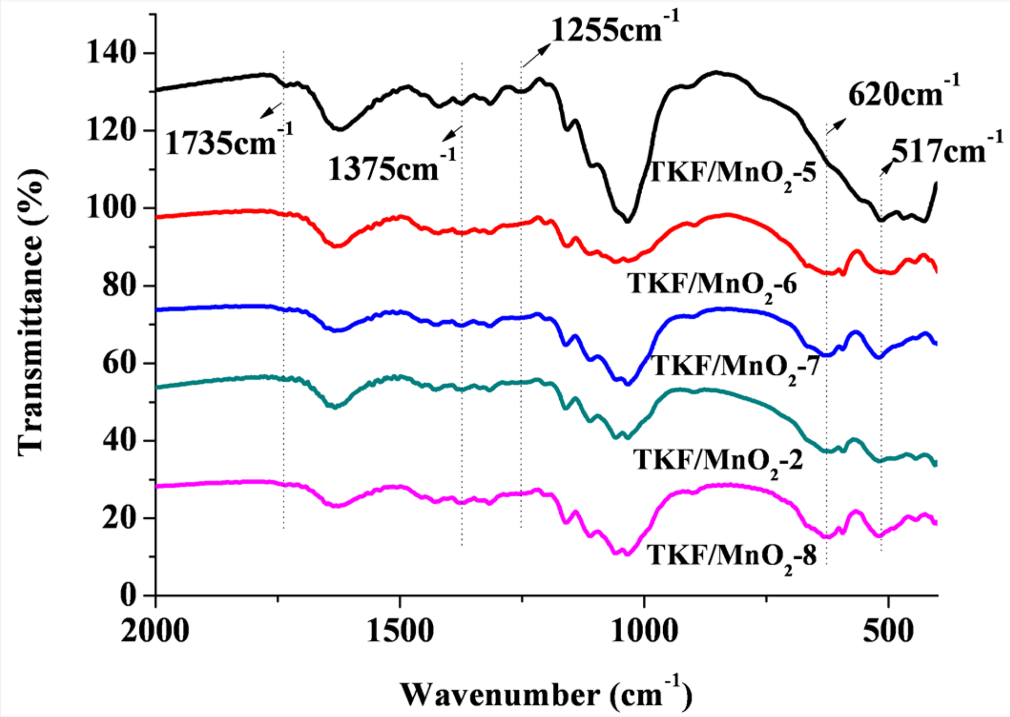

Fig.S3 FTIR spectra of TKF/MnO_2-5, TKF/MnO_2-6, TKF/MnO_2-7, TKF/MnO_2-2 and TKF/MnO_2-8 composites

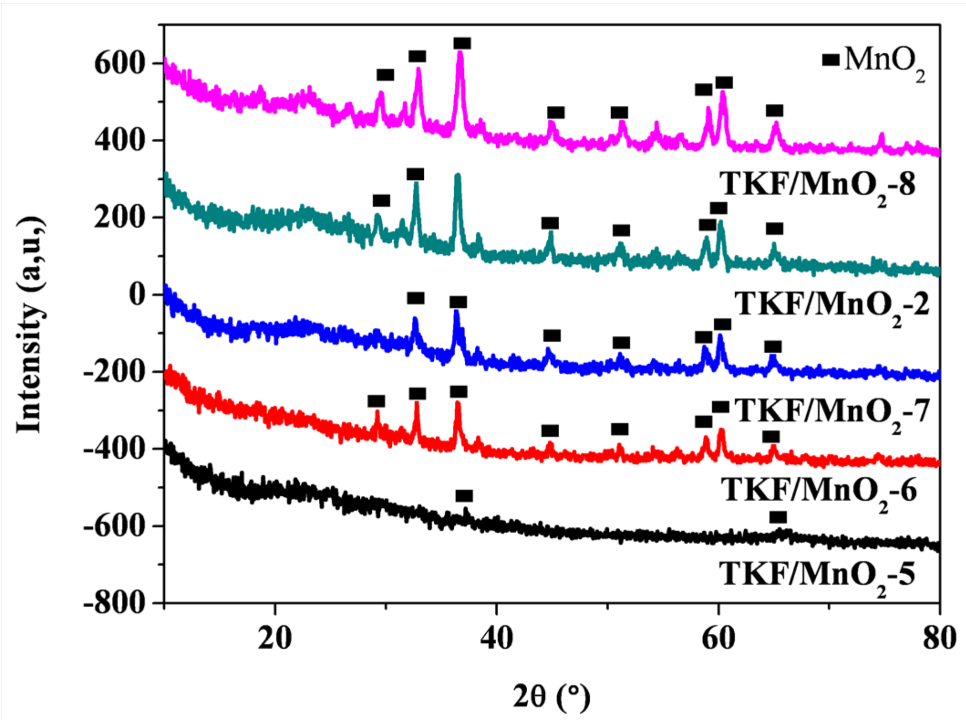

Fig.S4 XRD spectra of TKF/MnO_2-5, TKF/MnO_2-6, TKF/MnO_2-7, TKF/MnO_2-2 and TKF/MnO_2-8 composites

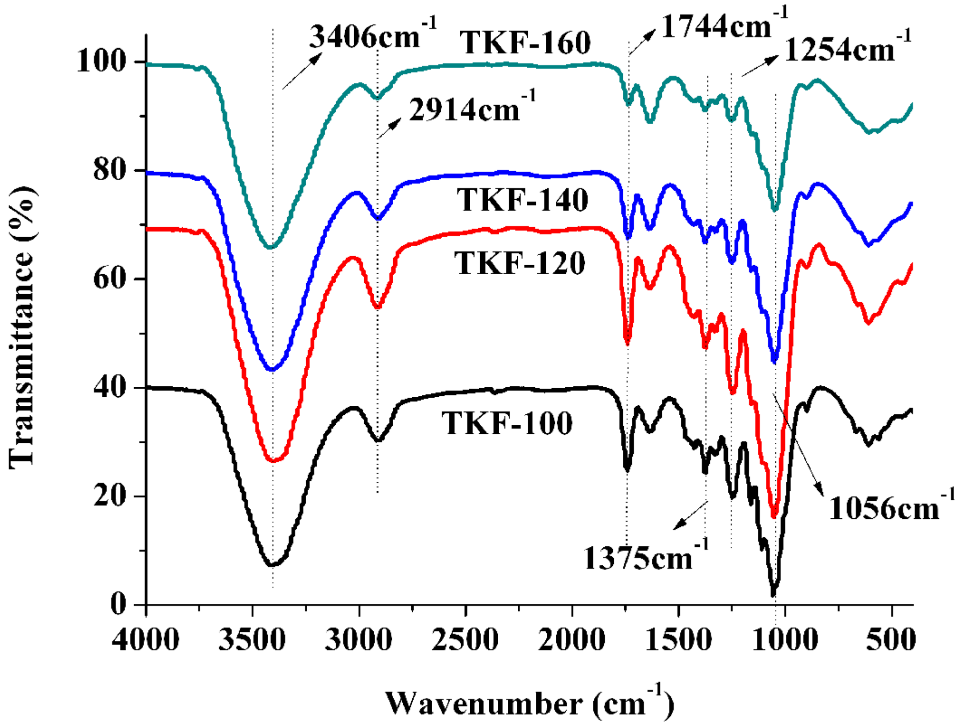

Fig.S5 FTIR spectra of TKF-100, TKF-120, TKF -140, and TKF-160

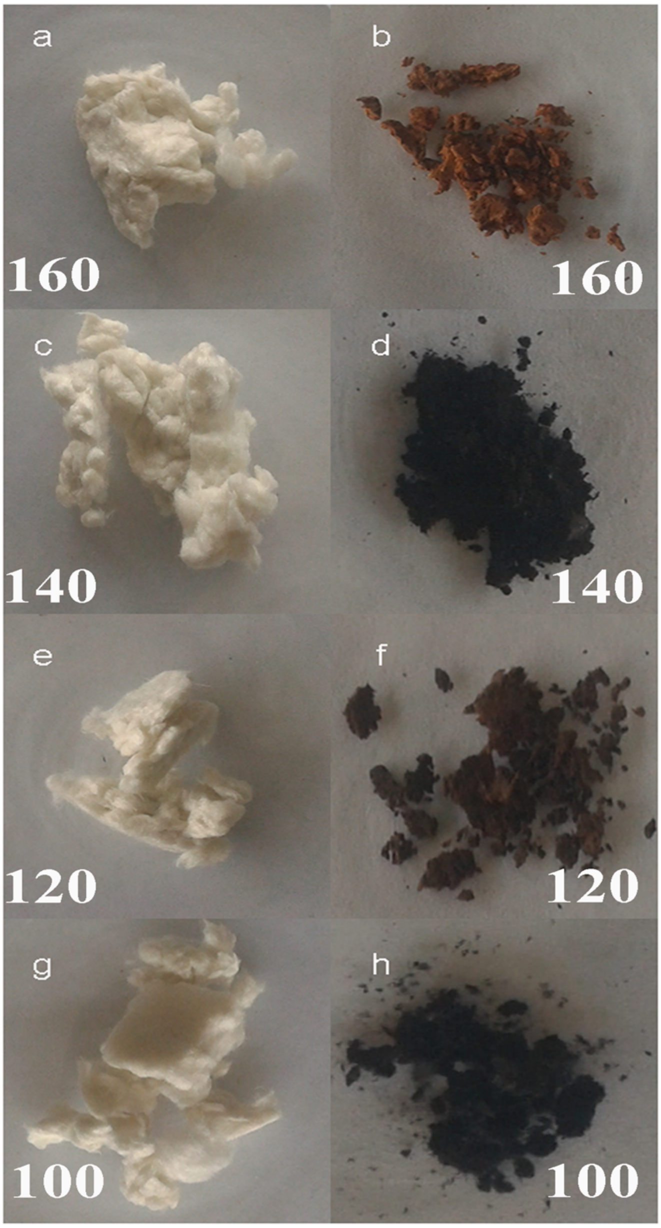

Fig.S6 Digital photos of the hydrothermally treated TKF and TKF/MnO_2 composites prepared at different hydrothermal temperature: (a) TKF-160, (b) TKF/MnO_2-11, (c) TKF-140, (d) TKF/MnO_2-6 (e) TKF -120, (f) TKF/MnO_2-10, (g) TKF-100, and (h) TKF/MnO_2-9

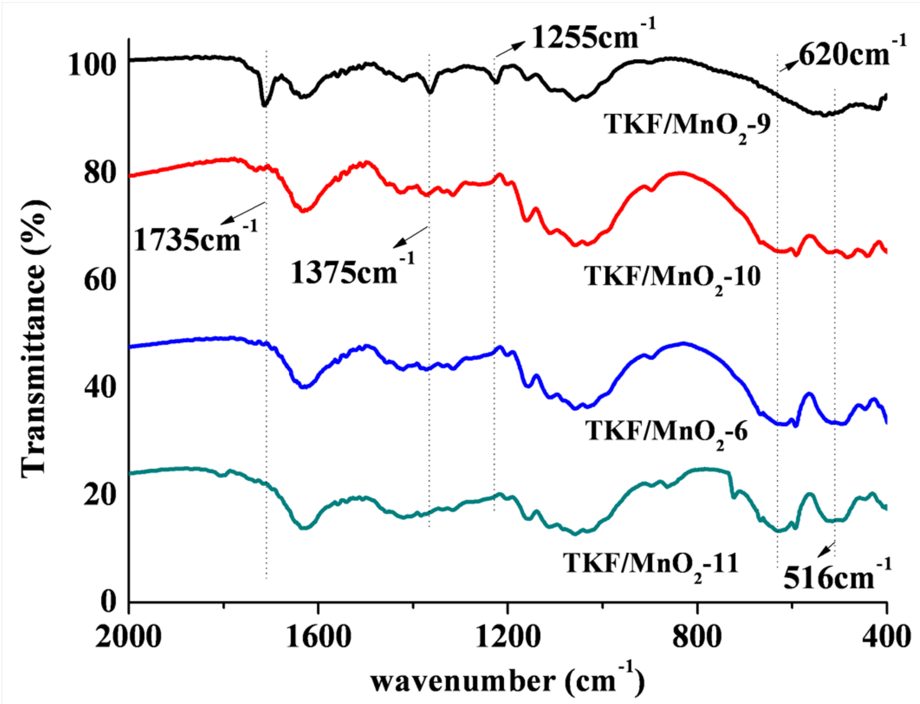

Fig.S7 FTIR spectra of TKF/MnO_2-6, TKF/MnO_2-9, TKF/MnO_2-10 and TKF/MnO_2-11 composites

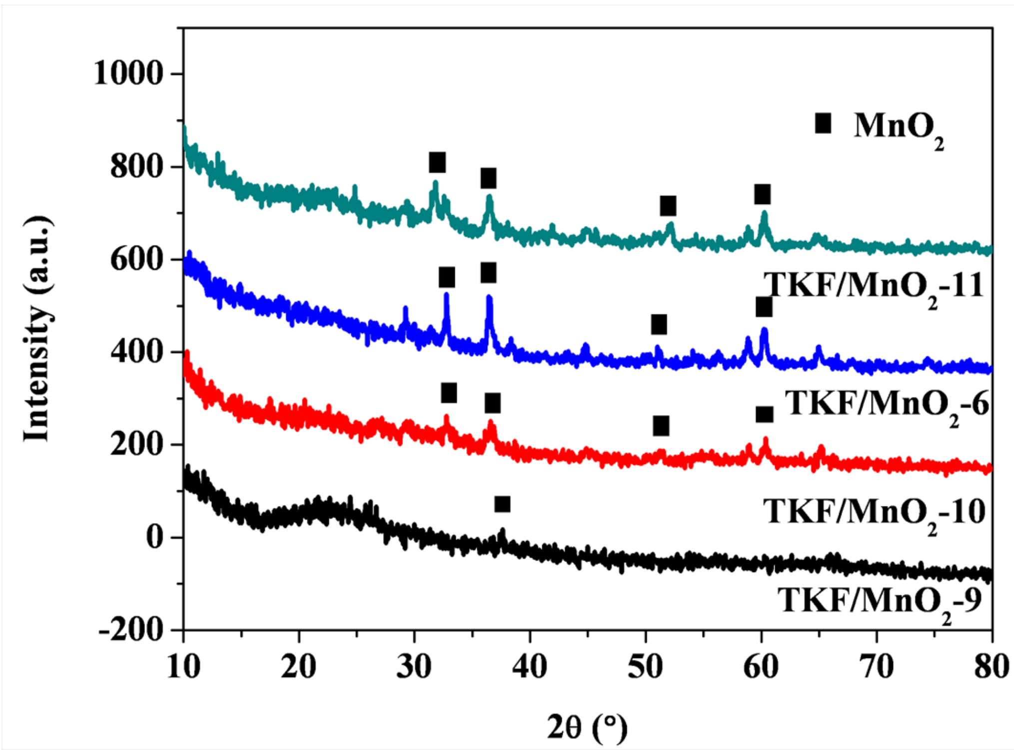

Fig.S8 XRD spectra of TKF/MnO_2-6, TKF/MnO_2-9, TKF/MnO_2-10 and TKF/MnO_2-11 composites

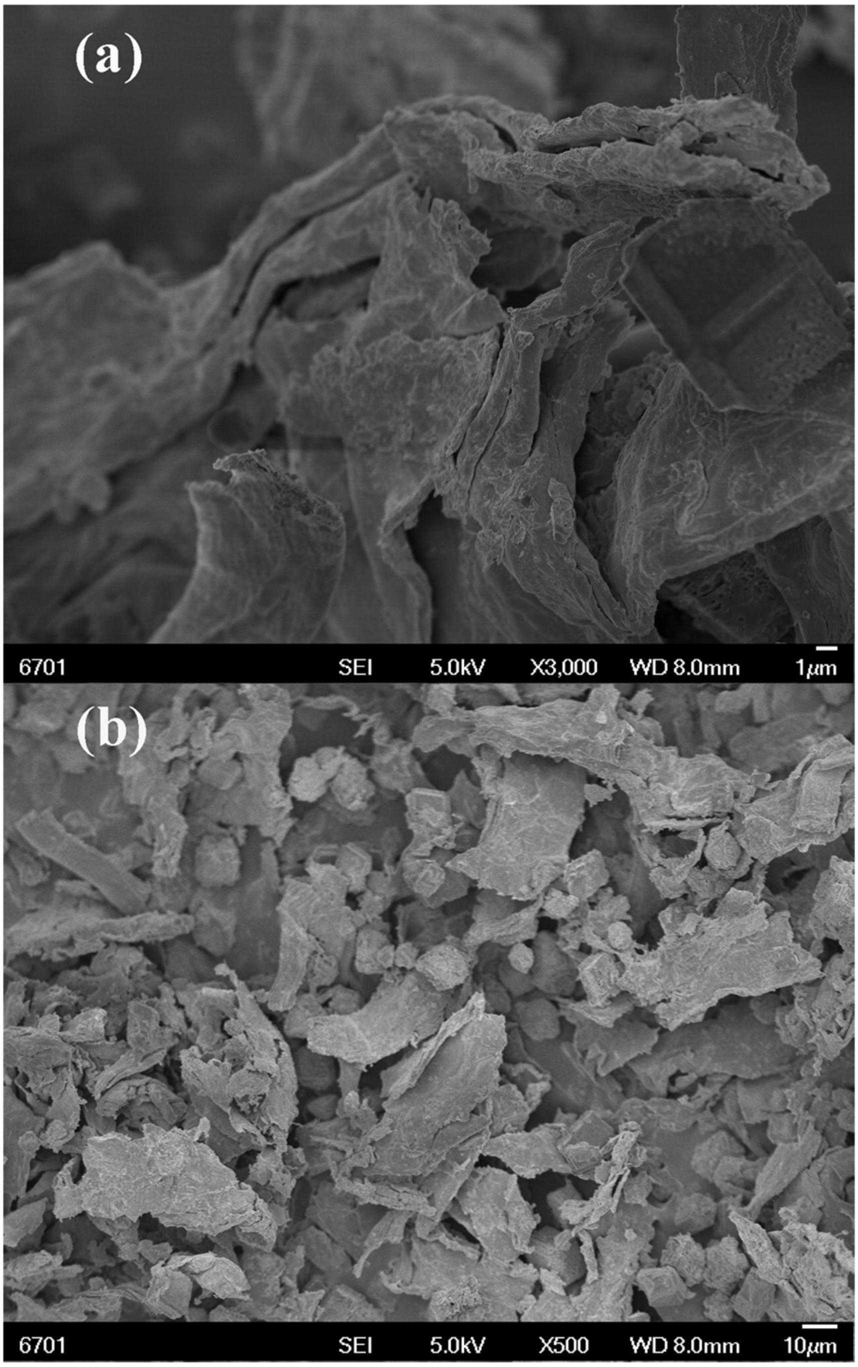

Fig.S9 SEM images of TKF/MnO_2-11

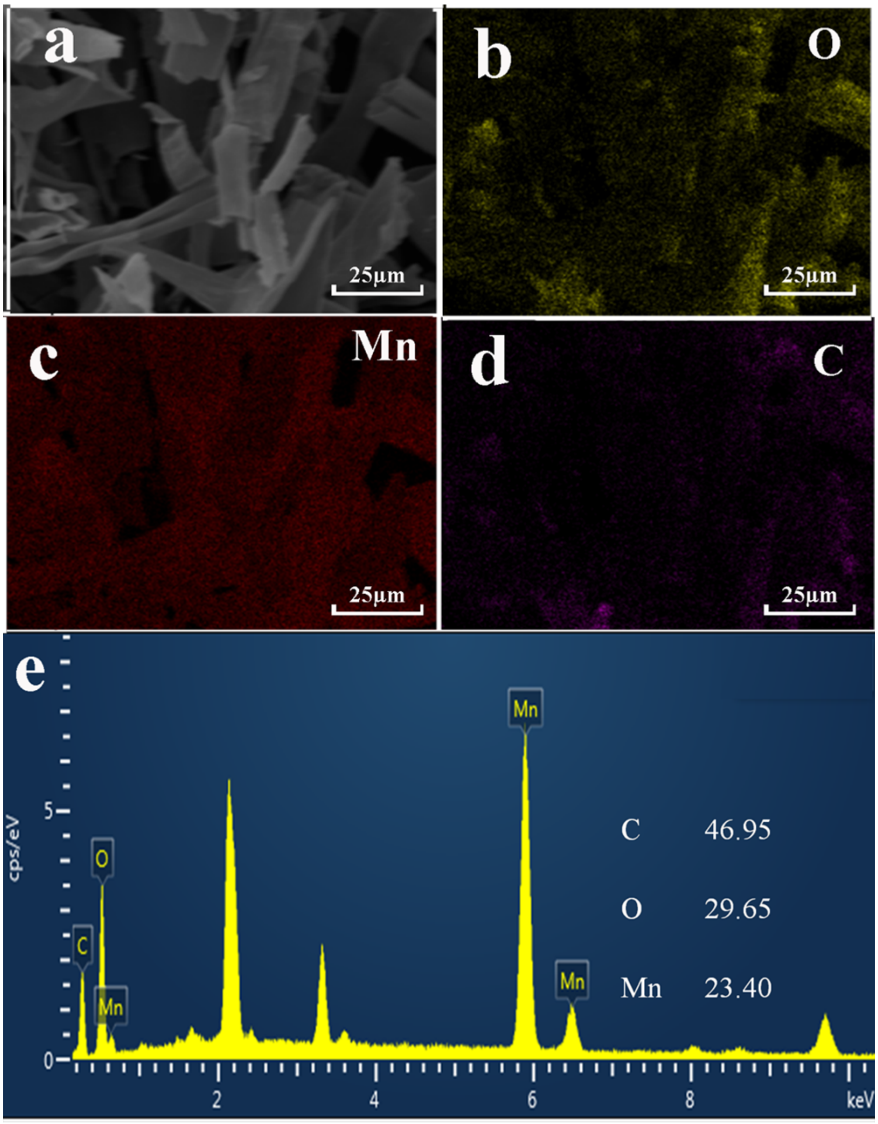

Fig.S10 (a-d) Element mapping images of TKF/MnO_2-5 (e) EDX pattern of TKF/MnO_2-5, the inset shows the atomic ratio of Mn, O and C

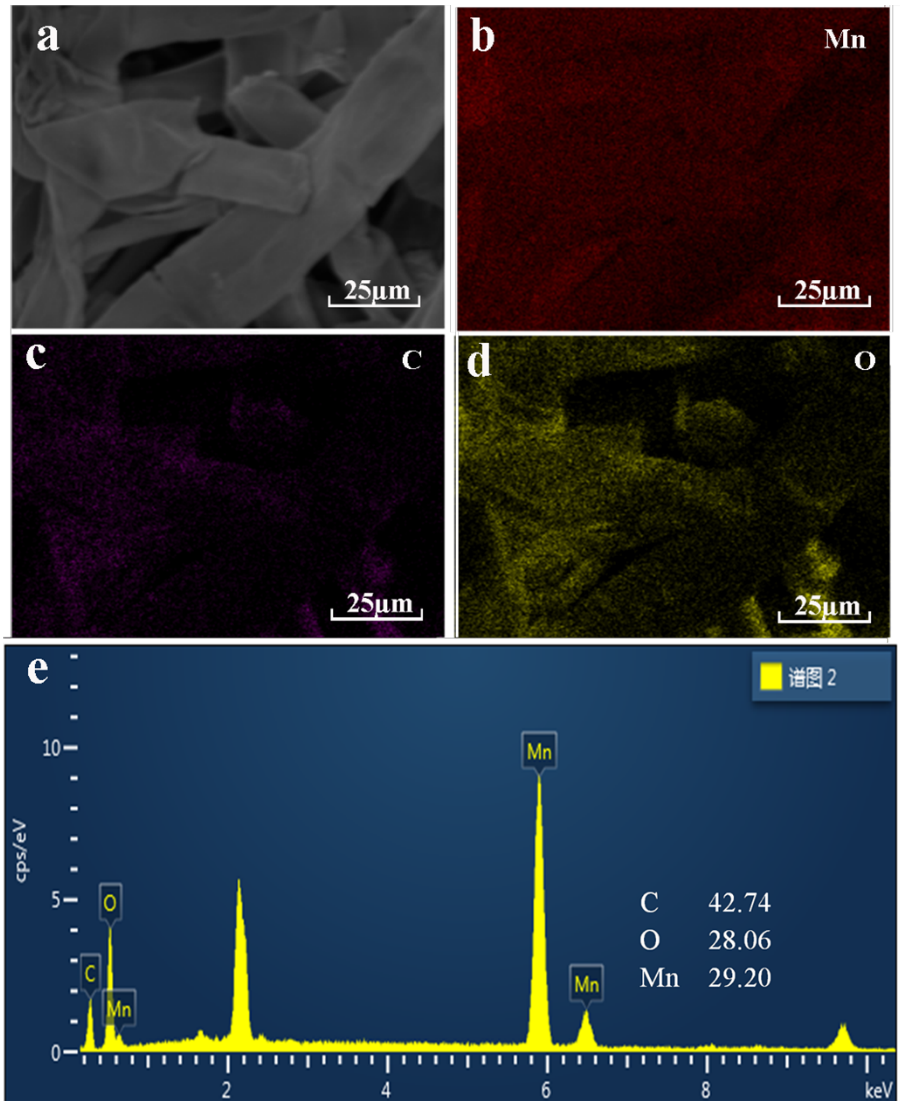

Fig.S11 (a-d) Element mapping images of TKF/MnO_2-7 (e) EDX pattern of TKF/MnO_2-7, the inset shows the atomic ratio of Mn, O and C

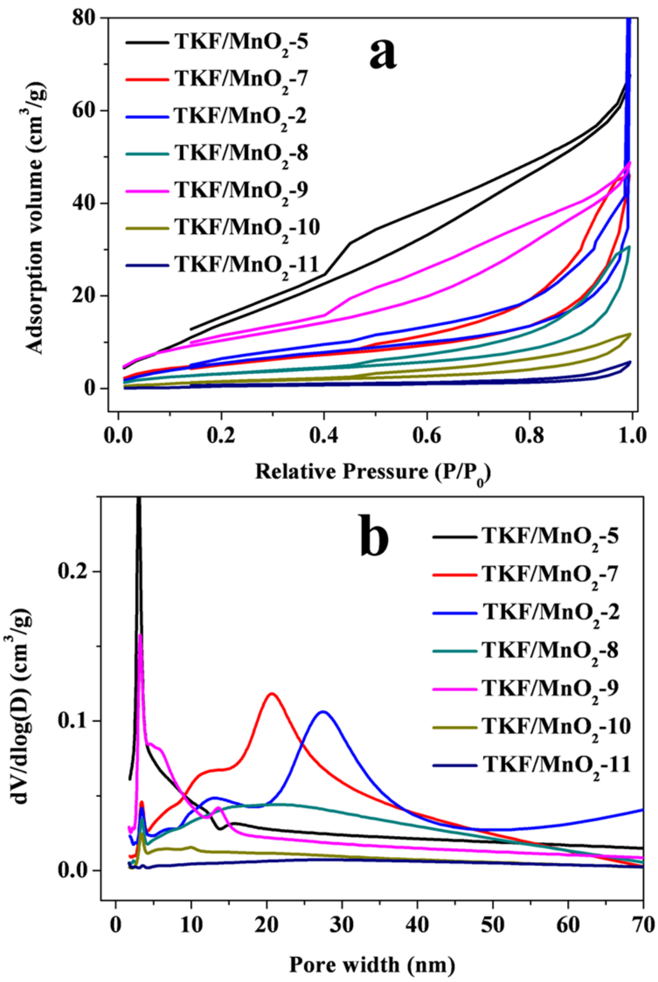

Fig.S12 (a) N_2 adsorption/desorption isotherms and (b) BJH pore size distribution of TKF/MnO_2-2, 5 ~ 11composites

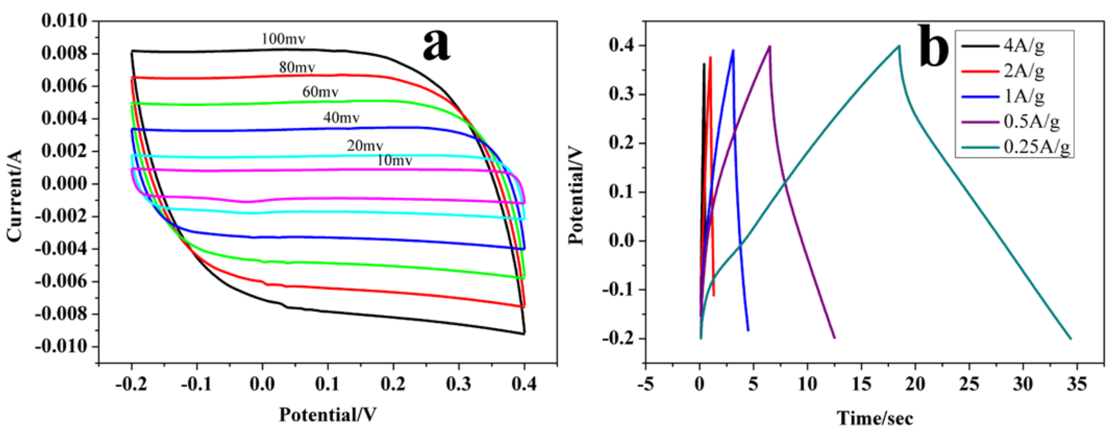

Fig.S13 (a) CV curves at different scan rates, (b) GCD curves at different current density for the TKF/MnO_2-2 composite in 1 M Na_2SO_4 electrolyte

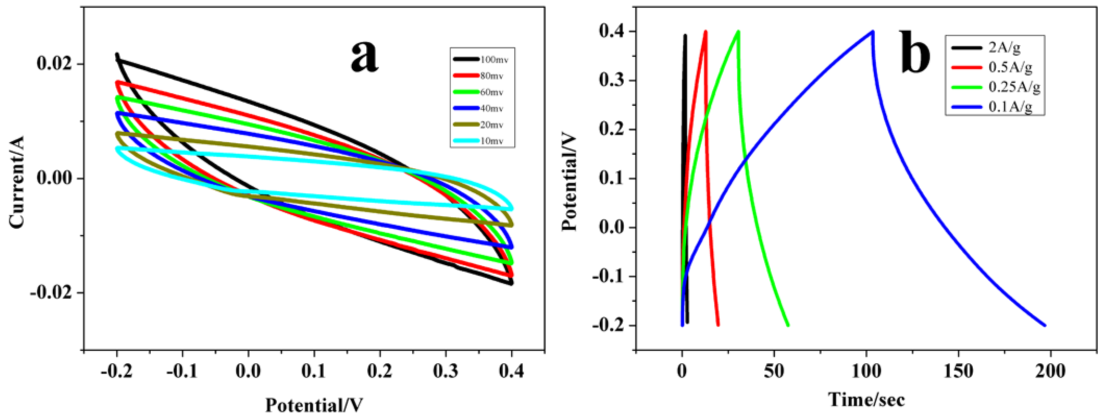

Fig.S14 (a) CV curves at different scan rates, (b) GCD curves at different current density for the TKF/MnO_2-5 composite in 1 M Na_2SO_4 electrolyte

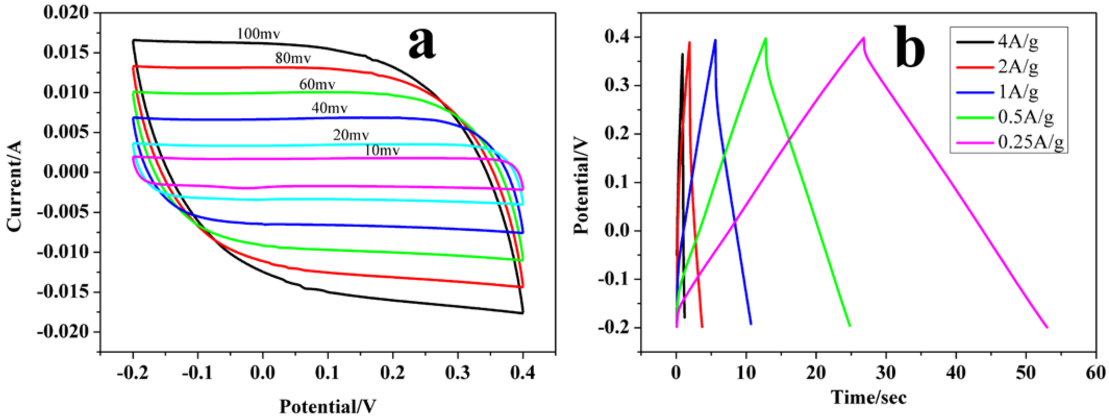

Fig.S15 (a) CV curves at different scan rates, (b) GCD curves at different current density for the TKF/MnO_2-7 composite in 1 M Na_2SO_4 electrolyte

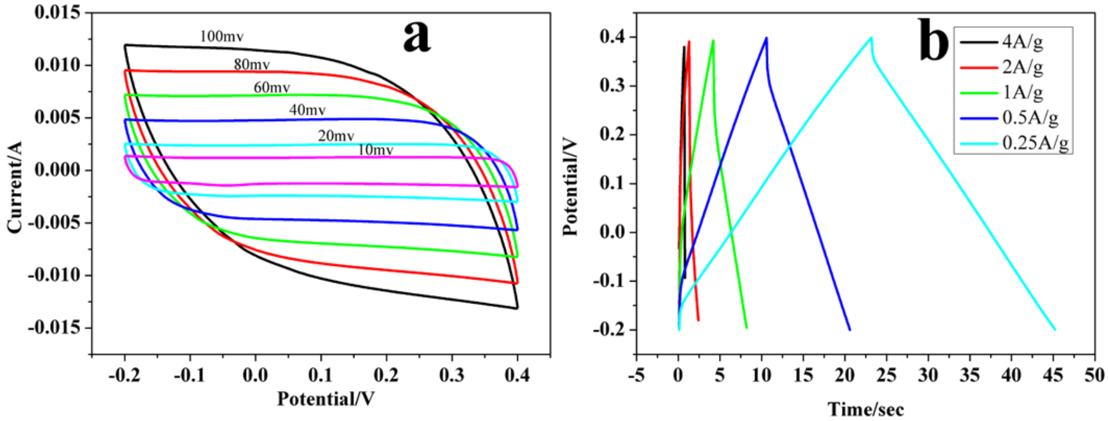

Fig.S16 (a) CV curves at different scan rates, (b) GCD curves at different current density for the TKF/MnO_2-8 composite in 1 M Na_2SO_4 electrolyte

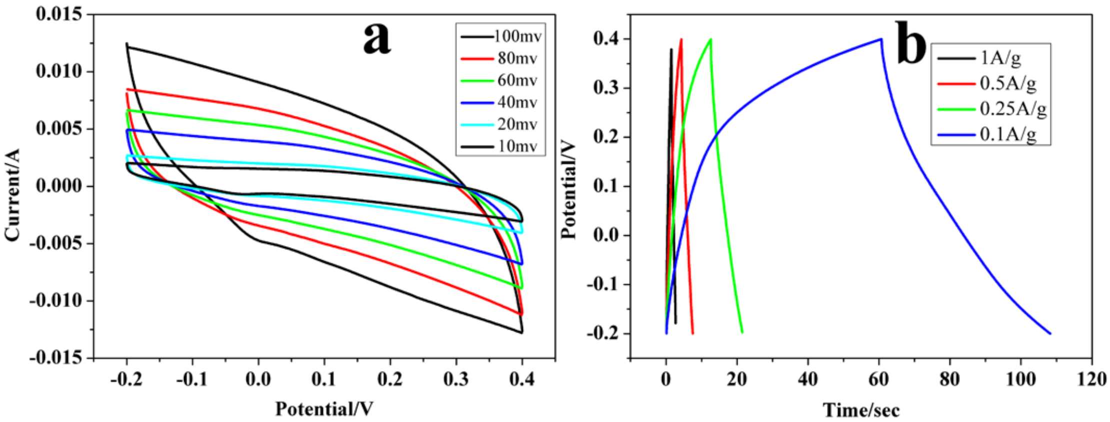

Fig.S17 (a) CV curves at different scan rates, (b) GCD curves at different current density for the TKF/MnO_2-9 composite in 1 M Na_2SO_4 electrolyte

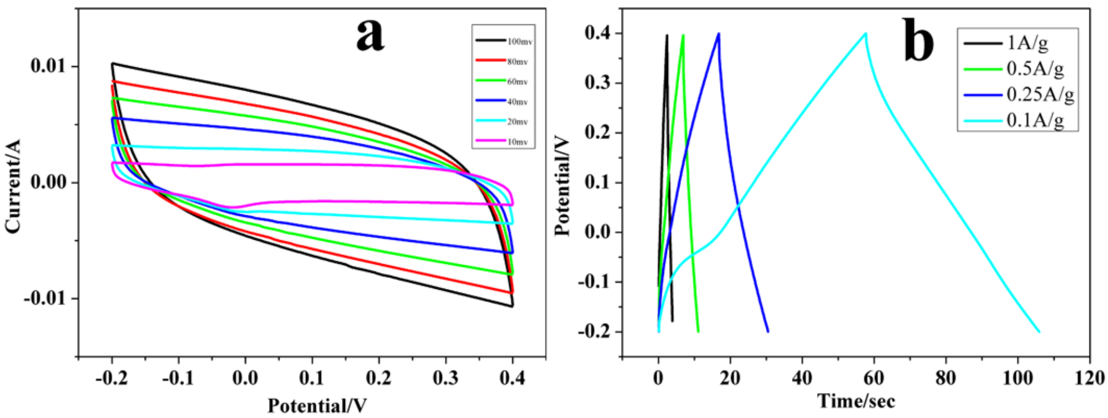

Fig.S18 (a) CV curves at different scan rates, (b) GCD curves at different current density for the TKF/MnO_2-10 composite in 1 M Na_2SO_4 electrolyte

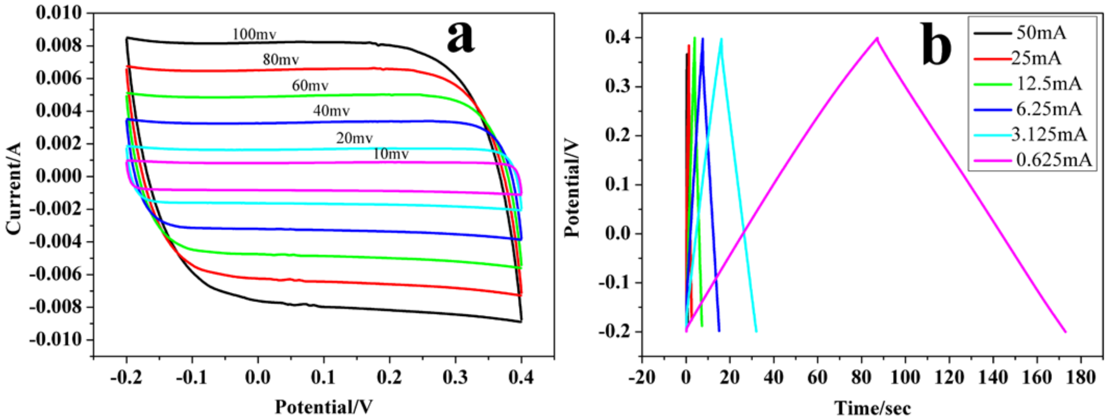

Fig.S19 (a) CV curves at different scan rates, (b) GCD curves at different current density for the TKF/MnO_2-11 composite in 1 M Na_2SO_4 electrolyte

Table S1. N_2 adsorption/desorption analyses of TKF and TKF/MnO_2 composites

Sample	$^{a}S_{BET}$ (m^2/g)	$^{b}S_{ext}$ (m^2/g)	$^{c}V_{tot}$(cm^3/g)
TKF	0.8875	-	0.0012
TKF/MnO_2-5	65.97	107.37	0.0941
TKF/MnO_2-6	222.41	261.93	0.4962
TKF/MnO_2-7	20.66	24.19	0.0520
TKF/MnO_2-2	18.19	34.51	0.0431
TKF/MnO_2-8	12.30	15.15	0.0335
TKF/MnO_2-9	6.63	9.32	0.0143
TKF/MnO_2-10	23.25	25.67	0.0681
TKF/MnO_2-11	39.15	47.00	0.0057

[a] BET (Brunauer-Emmett-Teller) surface area, [b] External surface area, calculated using *t*-plot method, [c] Total pore volume, measured at P/P_0 = 0.975

Table S2 Comparison of capacitive performance of the supercapacitors based on various Natural fiber composites presented in literature and the present work.

Sample	C_{max}	Ref
Cotton fiber/SWNT-MnO_2	210 F g^{-1}	[1]
Carbon fiber/MnO_2	0.41 F cm^{-2},	[2]
Carbon fiber/MnO_2	110 F g^{-1}	[3]
Textile fiber/graphene/MnO_2	315 F g^{-1}	[4]
Polyester fibers/CNT/MnO_2	2.8 F cm^{-2}	[5]
Carbon/MnO_2	190 F g^{-1}	[6]
Cotton fiber/ SWNT	70 F g^{-1}	[7]
Activated carbon textile/MnO_2	70 F g^{-1}	[8]
Cotton lawn	83 F g^{-1}	[9]
Cotton-based carbon fibers	355 F g^{-1}	[10]
Cotton fiber/PPy/LGS	304 F g^{-1}	[11]
Bacterial cellulose/PANI	273 F g^{-1}	[12]
Cellulose Fiber/CNT/MnO_2/CNT	290 F g^{-1}	[13]
Cotton fiber/PPy	268 F g^{-1}	[14]
Cellulose fiber/PANI/silver	176 mF/cm^2	[15]
Cellulose fiber/reduced graphene oxide/carbon nanotube	252 F g^{-1}	[16]
PPy-MnO_2-CNT-cotton	38.6 mF cm^{-2} (two electrode)	[17]
PPy/cotton fiber	52 F g^{-1}	[18]
PPy/bacterial cellulose	459.5 F g^{-1}.	[19]
Au/PPy cotton fabric	254.9 F g^{-1}	[20]
Kapok fiber/MnO_2	117 F g^{-1}	This work

C_{max}, maximum specific capacitance

1 L. B. Hu, M. Pasta, F. L. Mantia, L. F. Cui, S. Jeong , H. D. Deshazer, J. W. Cho, S. M. Han, Y. Cui, *Nano letters*, 2010, **10**,708-714.

2 X. Xiao, T. Q. Li, P. H. Yang, Y. Gao, H. Y. Jin, W. J. Ni, W. H. Zhan, X. H. Zhang, Y. Z. Cao, J. W. Zhong, L. Gong, W. C. Yen, W. J. Mai, J. Chen, K.F. Huo, Y. L. Chu, Z. L. Wang, J. Zhou, *Acs Nano*, 2012, **6**, 9200-9206.

3 A. E. Fischer, K. A. Pettigrew, D. R. Rolison, R. M. Stroud, J. W. Long, *Nano Letters*, 2007, **7**, 281-286.

4 G. H. Yu, L. B. Hu, M. Vosgueritchian, H. L. Wang, X. Xie , J. R. McDonough, X. Cui , Y. Cui, Z. N. Bao. *Nano letters*, 2011, **11**, 2905-2911.

5 L. B. Hu, W. Chen, X. Xie, N. Liu, Y. Yang, H. Wu, Y. Yao, M. Pasta, H. N. Alshareef, Y. Cui, *Acs Nano*, 2011, **5**, 8904-8913.

6 J. K. Chang, C. T. Lin, W. T. Tsai, *Electrochemistry communications*, 2004, **6**, 666-671.

7 M. Pasta, F. L. Mantia, L.B. Hu, H. D. Deshazer, Y. Cui, *Nano Research*, 2010, **3**, 452-458.

8 L. H. Bao, X, D. Li, *Advanced Materials*, 2012, **24**, 3246-3252.

9 K. Jost, C. R. Perez, J. K. McDonough, V. Presser, M. Heon, G. Dion, Y. Gogotsi, *Energy & Environmental Science*, 2011, **4**, 5060-5067.

10 S. G. Wang, Z. H. Ren, J. P. Li, Y. Q. Ren, L. Zhao, J. Yu. *RSC Advances*, 2014, **4**, 31300-31307.

11 L. G. Zhu, L. Wu, Y. Y. Sun, M. X. Li, J. Xu, Z.K. Bai, G. J. Liang, L. Liu, D. Fang, W. L. Xu C, *RSC Advances*, 2014, **4**, 6261-6266.

12 H. H. Wang, E. W. Zhu, J.Z. Yang, P. P. Zhou, D. P. Sun, W. H. Tang, *The Journal of Physical Chemistry C*, 2012, **116**, 13013-13019.

13 Z. Gui, H. L.Zhu, E. Gillette, X. G. Han, G. W. Rubloff, L. B. Hu, S. B. Lee, *ACS nano*, 2013, **7**, 6037-6046.

14 K. F. Babu, S. P. S. Subramanian, M. A. Kulandainathan, *Carbohydrate polymers*, 2013, **94**, 487-495.

15 X. D. Zhang, Z. Y. Lin, B. Chen, W. Zhang, S. Sharmad, W. T. Gu, Y. L. Deng, *Journal of Power Sources*, 2014, **246**, 283-289.

16 Q. F. Zheng, Z. Y. Cai, Z. Q. Ma, S. Q. Gong, *ACS applied materials & interfaces*, 2015, **7**, 3263–3271.

17 N. S. Liu, W. Z. Ma, J. Y. Tao, X. H. Zhang, J. Su, L.Y. Li, C. X. Yang, Y. H. Gao, D. Golberg, Y. Bando, *Advanced Materials*, 2013, **25**, 4925-4931.

18 G. J. Liang, L. G. Zhu, J. Xu, D. Fang, Z. K. Bai, W. L. Xu, *Electrochimica Acta*, 2013, **103**, 9-14.

19 J. Xua, L. G. Zhu, Z. K. Bai, G. J. Liang, L. Liu, D. Fang, W. L. Xu, *Organic Electronics*, 2013, **14**, 3331-3338.

20 B. B. Yue, C. Y. Wang, X. Ding, G. G. Wallace, *Electrochimica Acta*, 2013, **113**, 17-22.